

A simple method to detect cracks in beam-like structures

Jiawei Xiang^{*1,2}, Toshiro Matsumoto¹, Jiangqi Long², Yanxue Wang³ and Zhansi Jiang³

¹Department of Mechanical Science and Engineering, Nagoya University, Furo-cho,
Chikusa-ku, Nagoya, 464-8603, Japan

²College of Mechanical and Electrical Engineering, Wenzhou University, 325035, China

³School of Mechanical and Electrical Engineering, Guilin University of Electronic Technology, Guilin,
541004, China

(Received December 15, 2011, Revised March 5, 2012, Accepted March 12, 2012)

Abstract. This study suggests a simple two-step method for structural vibration-based health monitoring for beam-like structures which only utilizes mode shape curvature and few natural frequencies of the structures in order to detect and localize cracks. The method is firstly based on the application of wavelet transform to detect crack locations from mode shape curvature. Then particle swarm optimization is applied to evaluate crack depth. As the Rayleigh quotient is introduced to estimate natural frequencies of cracked beams, the relationship of natural frequencies and crack depths can be easily obtained with only a simple formula. The method is demonstrated and validated numerically, using the numerical examples (cantilever beam and simply supported shaft) in the literature, and experimentally for a cantilever beam. Our results show that mode shape curvature and few estimated natural frequencies can be used to detect crack locations and depths precisely even under a certain level of noise. The method can be extended for health monitoring of other more complicated structures.

Keywords: beam-like structures; rayleigh quotient; wavelet transform; natural frequency estimation; crack detection; particle swarm optimization

1. Introduction

Vibration-based crack detection methods are global non-destructive testing methods, which are based on the fact that any changes introduced in a structure (including cracks) change its physical properties, which in turn change the structural mode parameters (natural frequency, mode shape, damping). These methods use the changes in the structural mode parameters extracted from vibration response of cracked structure for the purposes of crack detection (Fan and Qiao 2011). There are different strategies suggested for vibration-based crack detection purposes depending on the type of the mode parameters used: natural frequency, mode shape or damping. All of these have their advantages and disadvantages (Fan and Qiao 2011). Because modal damping cannot be measured easily, natural frequencies and mode shape are commonly used to detect cracks in structures.

Crack detection methods that are based on the first few natural frequencies of a structure present a very attractive possibility since these are quite easy to obtain from experiment (Chen *et al.* 2005). Therefore, the model-based crack detection methods associated with frequency measurement have

*Corresponding author, Professor, E-mail: wxx8627@163.com

drawn special attention in the open accessible literature (Chaudhari and Maiti 2000, Dong *et al.* 2009, Lele and Maiti 2002, Li *et al.* 2005, Li and He 2011, Liang *et al.* 1991, 1992a,b, Hu and Liang 1993, Maiti and Patil 2004, Nandwana and Maiti 1997, Ostachowicz and Krawczuk 1991, Papadopoulos and Dimarogonas 1987, Patil and Maiti 2003, 2005, Shih *et al.* 2009, 2011, Sinou 2007). Generally, there are two procedures to accomplish the crack detection in structures. The first procedure is forward problem analysis, which considers the construction of a cracked stiffness matrix exclusively for the crack section and the computation of crack detection database for dynamic parameters. The cracks require a large number of refined elements in the local areas and thus complicate the computational process. Therefore, wavelet finite element method with reduced number of elements was proposed to detect cracks in beams (Chen *et al.* 2006, Li *et al.* 2005, Li and He 2011, Xiang *et al.* 2007a, 2008, 2009, Xiang and Liang 2011) with complex procedure. The second procedure is the inverse problem analysis, which measures first few natural frequencies and search for crack location and depth from the damage detection database, i.e., the relationship of natural frequencies and crack parameters (locations and depths). However, so far only the single-crack detection methods are well established and crack detection software is also reported (Xiang *et al.* 2011). The reason is that the natural frequency alone cannot provide enough information for multiple crack detection (Fan and Qiao 2011). A confounding factor which limits the application of the lower natural frequencies is that crack is typically a local phenomenon while the first few natural frequencies capture the global structural response. Local response is captured by higher frequencies which are more difficult to excite and measure. Thus many researchers intended to increase the sensitivity of the lower frequency structural response to crack (Gokdag, 2011, Kim *et al.* 2008, Koo *et al.* 2008, Lakshmanan *et al.* 2008, Mendrok and Uhl 2010, Montejo, 2011). Moreover, to solve the ill-posed inverse problem of crack detection, some intelligent computational techniques, such as genetic algorithms (GAs), Particle swarm optimization (PSO) and neural networks (NNs), etc., are proposed to detect cracks in structures (Amiri *et al.* 2011, Begambre and Laier 2009, Kim *et al.* 2007, Yun *et al.* 2009).

Singularity detection from mode shape is attractive mainly because it is possible to identify the existence and locations of cracks based on the priori knowledge of the cracked zones (Gokdag 2010, Rajasekaran and Varghese 2005). Certain mode shape associated with cracked beam structures contains local singularity information. However, the singular locations from arbitrary mode shape (especially the easily measured first mode shape) can not be easily observed even if the wavelet transform is employed to extract local singularity characteristics. Therefore, for a well selected mode shape (act as original signal), the wavelet coefficients are calculated and plotted in the full region for each level of the wavelets. Then the distribution of the wavelet coefficients at each level is examined and the peaks or sudden changes in the wavelet coefficients will pinpoint the crack locations. To detect crack depths, mode shape may not yield reliable results when there existence of measurement errors. Therefore, in order to improve the effectiveness for crack location detection using only the arbitrary mode shape, mode shape curvature (Pandey 1991) might be a good candidate.

To calculate the natural frequency of a structure with cracks there could be an existing estimation formula. It is not necessary to use the finite element method or other complex numerical methods (such as the wavelet finite element method). This research is motivated by the need for a simple method to estimate the natural frequency of structures with cracks. Therefore, the purpose of the present work is to establish a simple method to detect and localize cracks in beam-like structures using mode shape curvature and few natural frequencies. With this method, we use wavelet

transform to decompose mode shape curvature to localize cracks. Then the Rayleigh quotient is employed to estimate the approximate natural frequencies and the relationship of natural frequencies and crack depths can be easily constructed by a simple formula. Different boundary conditions of rectangle cross-section beam and shaft are considered in the present investigation. The resulting crack depth detection inverse problems are then solved by PSO using the first few natural frequencies as the inputs. The simulation results are compared with literature and the precision of the present method is examined. The performance of this method has also been examined using experimental data of a cantilever beam. The detection result shows that the proposed method can be applied to real structures. The rest of the paper is organized as follows. The next section introduces the approximate formulas to calculate natural frequencies. Section 3 introduces the background of the suggested methodology. Then a simple method for defect detection and localizations is suggested. Numerical simulations and experimental investigation are presented in sections 4 and 5, respectively.

2. Natural frequencies estimation formulas

Fig. 1 shows a beam or shaft with some damages on its surface. The cracked cross-section in beam with rectangle and circular cross-sections are shown in Figs. 2(a) and (b), respectively. $\beta_i = x_i / L$, ($i=1,2,\dots, n$) denotes the normalized location of crack i in beam, and L is the beam length.

For a beam with rectangular cross-section, each crack can be represented by a rotational spring with stiffness k_i is defined by (Ostachowicz and Krawczuk 1991).

$$k_i = bh^2E/(72\pi\alpha_i^2f(\alpha_i)) \tag{1}$$

in which the experimental formula $f(\alpha_i)$ is (Tada *et al.* 2000)

$$f(\alpha_i) = 0.6384 - 1.035\alpha_i + 3.7201\alpha_i^2 - 5.1773\alpha_i^3 + 7.553\alpha_i^4 - 7.332\alpha_i^5 + 2.4909\alpha_i^6 \tag{2}$$

where $\alpha_i = c_i / h$ ($i = 1,2,\dots, n$) denotes normalized crack depth as shown in Fig. 2(a). E is Young's modulus, b is the beam width, and h is the beam height.

For a beam with circular cross-section, each crack can be represented by a rotational spring with stiffness k_i is calculated by considering a combination of a series of thin strip as (Papadopoulos and

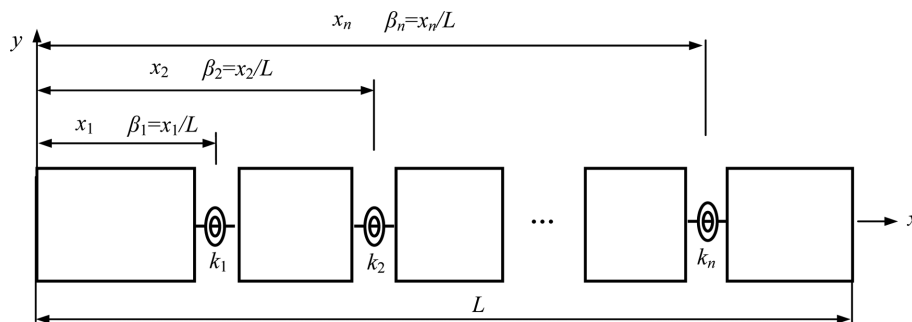


Fig. 1 A beam or shaft with n cracks on its surface

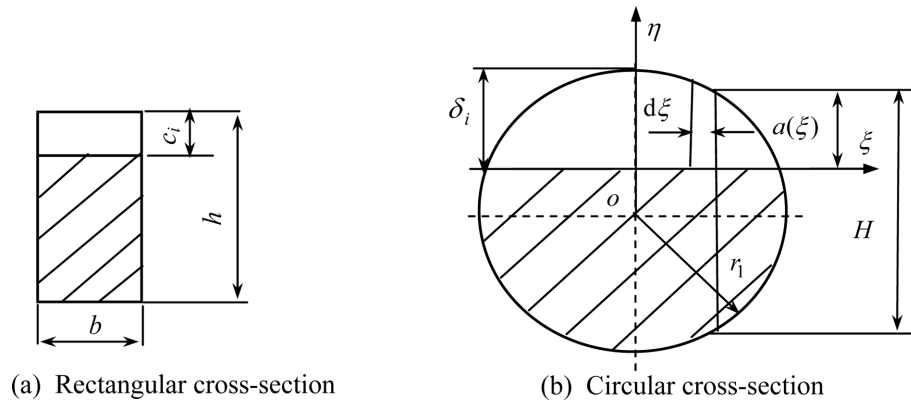


Fig. 2 Cracked rectangular and circular beam cross-sections

Dimarogonas 1987).

$$k_i = \frac{\pi E r_1^8}{32(1-\mu)} \frac{1}{\int_{-r_1\sqrt{1-(1-2\alpha_i)^2}}^{r_1\sqrt{1-(1-2\alpha_i)^2}} (r_1^2 - \xi^2) \left[\int_0^{a(\xi)} \eta F^2(\eta/H) d\eta \right] d\xi} \quad (3)$$

where δ_i is crack depth, μ is the Poisson's ratio, the normalized crack depth for circular cross-section beam is $\alpha_i = \delta_i / 2r_1$, the crack depth of a thin strip is $a(\xi) = 2r_1\alpha_i - (r_1 - \sqrt{r_1^2 - \xi^2})$, the height of thin strip is $H = 2\sqrt{r_1^2 - \xi^2}$, and the function $F(\eta/H)$ is given by the following experimental formula (Tada *et al.* 2000).

$$F(\eta/H) = 1.122 - 1.40(\eta/H) + 7.33(\eta/H)^2 - 13.08(\eta/H)^3 + 14.0(\eta/H)^4 \quad (4)$$

According to linear elastic fracture mechanics theory, the decrease in the strain energy of n cracks under m th modal vibration is equal to the energy stored in the fictitious rotational spring, which can be expressed in the form (Ostachowicz and Krawczuk 1991).

$$\Delta U_m = U_m - \bar{U}_m = \sum_i^n \frac{M_{mi}^2}{2k_i} \quad (5)$$

where \bar{U}_m is the strain energy of cracked beam containing n cracks, U_m is the strain energy of intact beam, which can be calculated based on Euler beam theory as

$$U_m = \frac{1}{2} \int_0^L EI \left(\frac{d^2 y_m}{dx^2} \right)^2 dx \quad (6)$$

and M_{mi} ($i = 1, 2, \dots, n$) is the bending moment at the crack location, i.e.

$$M_{mi} = EI \frac{d^2 y_m(x_i)}{dx^2} \quad (7)$$

in which y_m represent the m th mode shape of intact beam, I is the moment of inertia.

According to the assumption that the volume is a tiny loss of materials between intact and cracked beams, hence there is negligible difference between the kinetic energy of the beam with and without cracks. That is

$$T_m = \bar{T}_m = \frac{\rho A}{2} \int_0^l \left(\frac{dy}{dt} \right)^2 dx \quad (8)$$

where T_m and \bar{T}_m represent the kinetic energy of intact and cracked beam, respectively, A is the area of cross-section, and ρ is the mass density.

The natural angular frequency ω_m (for intact beam and the corresponding natural frequency $f_m = \omega_m/2\pi$) and $\bar{\omega}_m$ (for beam with n cracks and the corresponding natural frequency $\bar{f}_m = \bar{\omega}_m/2\pi$) can be approximate evaluated with Rayleigh quotient as

$$\omega_m^2 = \frac{U_m}{T_m} \quad (9)$$

and

$$\bar{\omega}_m^2 = \frac{\bar{U}_m}{\bar{T}_m} \quad (10)$$

Therefore, consideration of Eq. (5) to Eq. (10) and $f_m + \bar{f}_m \cong 2f_m$, we have

$$\frac{f_m^2 - \bar{f}_m^2}{f_m^2} = \frac{\omega_m^2 - \bar{\omega}_m^2}{\omega_m^2} = \left(\frac{U_m - \bar{U}_m}{T_m} \right) / \left(\frac{U_m}{T_m} \right) \quad (11)$$

$$\Rightarrow \frac{(f_m + \bar{f}_m)(f_m - \bar{f}_m)}{f_m^2} = \sum_i^n \frac{M_{mi}^2}{2k_i} / U_m = EI / \int_0^L \left(\frac{d^2 y_m}{dx^2} \right)^2 dx \sum_{i=1}^n \frac{\left[\frac{d^2 y_m(x_i)}{dx^2} \right]^2}{k_i} \quad (12)$$

$$\Rightarrow \bar{f}_m \cong f_m \left\{ 1 - \phi_m \sum_{i=1}^n \frac{[v_m(x_i)]^2}{k_i} \right\} \quad (13)$$

where the constant term ϕ_m is defined as

$$\phi_m = \frac{EI}{2 \int_0^L (v_m)^2 dx} \quad (14)$$

and v_m is the m th curvature at the cross-section and defined as

$$v_m = \frac{d^2 y_m}{dx^2} \quad (15)$$

From Eq. (13), we can see clear that the m th natural frequency \bar{f}_m can be approximate calculated by rotational spring stiffness k_i ($i = 1, 2, \dots, n$) when the natural frequency f_m and the mode shape y_m of intact beam are known. For a uniform beam with various boundary conditions, the close-from

solutions of both f_m and y_m are given in handbooks (Harris and Piersol 2002, Timoshenko 1974). Therefore, the m th natural frequency f_m can be approximating estimated easily. It is note that f_m can be calculated by

$$f_m = \frac{(\lambda_m L)^2}{2\pi} \sqrt{\frac{EI}{\rho A L^4}} \quad (16)$$

where $\lambda_m L$ is the roots of the frequency equation for bending vibration of beams (Harris and Piersol 2002, Timoshenko 1974).

Take the simply supported beam at two ends (Pinned-pinned) for example, the roots of the frequency equation is

$$\lambda_m L = m\pi \quad (17)$$

and the m th mode shape y_m is

$$y_m = C_m \sin(\lambda_m x) \quad (18)$$

where C_m is a constant.

Submit Eq. (17) into Eq. (16), we have

$$f_m = \frac{m^2 \pi}{2L^2} \sqrt{\frac{EI}{\rho A}} \quad (19)$$

Submit Eqs. (17)-(19) into Eq. (13), we finally have

$$\bar{f}_m \cong \frac{m^2 \pi}{2L^2} \sqrt{\frac{EI}{\rho A}} \left(1 - \frac{EI}{L} \sum_{i=1}^n \frac{\sin^2(m\pi x_i/L)}{k_i} \right) \quad (20)$$

For other boundary conditions, such as Fixed-free (Cantilever), Fixed-fixed, Free-free, Fixed-pinned, Fixed-sliding, Pinned-free, etc., the expression of \bar{f}_m is much more complex. Therefore, according to Eq. (13), we use MATLAB Symbolic Math Toolbox (Higham and Higham 2005) to calculate \bar{f}_m .

3. Crack detection method

The method has been developed takes advantage of both wavelet transform and Particle Swarm Optimization (PSO) algorithm to detect crack locations and depths, respectively. Wavelet transform are particularly well suited to the singularity detection of signal masked by noise. Consider the mode shape curvature as signal, it is possible to detect how many cracks are available in beams and further determine the crack locations.

PSO is a heuristic method proposed by Kennedy, Eberhart and Shi (Kennedy and Eberhart 1995, Shi and Eberhart 1998). PSO searches for the optimal solutions without relying on the prior knowledge or properties of the problem being optimized. The applications for structural engineering problems (Fourie and Groenwold 2002, Zhong and Ye 2009, Begambre and Laier 2009) have demonstrated the reliability of the PSO method in locating optimal or near optimal solutions. It is also demonstrated that PSO can obtain better results in a faster, cheaper way compared with other methods. It is noteworthy that the relationship of natural frequencies and crack depths (crack depth

detection database) can be easily constructed using Eq. (13) if the crack locations are known (detected by wavelet transform from mode shape curvature). Therefore, the PSO algorithm can apply to detect crack depths from crack depth detection database if the few natural frequencies of cracked beam are measured.

The simple method is introduced in section 3.1 to section 3.3.

3.1 Detect crack locations

Measure the m th mode shape Y_m of the cracked beam-like structures by experimental modal analysis (EMA) and calculate the m th mode shape curvature V_m .

If the m th mode shape Y_m is measured, each point $V_{m,j}$ of mode shape curvature V_m are obtained numerically from the m th mode shape using a central difference approximation as (Pandey *et al.* 1991).

$$V_{m,j} = \frac{Y_{m,j+1} - 2Y_{m,j} + Y_{m,j-1}}{h_c^2} \quad (21)$$

where h_c is the length of the two neighbor nodes, j is the node at different spatial locations, $Y_{m,j-1}$, $Y_{m,j}$ and $Y_{m,j+1}$ are the three continuous nodes of Y_m .

Observed the peaks from arbitrary mode shape curvature.

Crack locations can be observed from arbitrary mode shape curvature. Obviously, if the peaks or sudden changes are not available, it means that no cracks are available in beams.

3.2 Evaluate crack depths

(1) Construct crack depth detection database using Eq. (13)

This procedure is called forward problem analysis in the literature. Because the crack singularity property, many numerical simulation methods, such as finite element method (FEM), wavelet FEM, adaptive FEM and the boundary element method (BEM) are employed to calculate the database (Chaudhari and Maiti 2000, Dong *et al.* 2009, Lele and Maiti 2002, Li *et al.* 2005, Li and He 2011, Maiti and Patil 2004, Nandwana and Maiti 1997, Patil and Maiti 2003, 2005, Xiang *et al.* 2007a, 2008). In the present, due to the Rayleigh quotient is employed to estimate natural frequencies, the relationship of natural frequencies and crack depths (crack depth detection database) can be easily constructed by a simple formula, i.e., Eq.(13). Hence, we continuously computing the first few natural frequencies versus different depths α_i ($i = 1, 2, \dots, n$) for the known normalized crack location β_i ($i = 1, 2, \dots, n$), as follows

$$\bar{f}_m = F_m(\alpha_1, \alpha_2, \dots, \alpha_n) \quad (m = 1, 2, \dots, q \geq n) \quad (22)$$

where F_m denote the relationship of crack depths $\alpha_1, \alpha_2, \dots, \alpha_n$ and the corresponding natural frequencies \bar{f}_m ($m = 1, 2, \dots, q$). In order to evaluate n crack depths in beam-like structure, the least q should be equals to n . Eq. (22) is also called the crack depth detection database.

To make a clearly description on how to construct crack depth detection database, we summarised as follows:

(a) Calculate k_i for different crack depths using Eq. (1) (for rectangle cross-section) or Eq.(3) (for circular cross-section).

(b) Use natural frequencies estimation equation Eq. (13) (for a simply supported beam/shaft, Eq. (13) is becoming Eq. (20)) to calculate natural frequencies of cracked structure with different depths.

(c) Obtain first few natural frequencies versus different depths, as shown in Eq. (22).

(d) The above is the forward analysis of crack depths detection (crack detection database). To decrease the errors between the calculated and measurement, we introduce the model updating technique, as proposed in Section 3.3.

It worth to point out that the existence of crack also influences axial and lateral stiffness of beams. However, if we only measure the vertical response of the beam, the coupling effect is very small and can be omitted because the three directions are perpendicular to each other.

Therefore, we seek the crack depths from the crack detection database using the measured few natural frequencies, as show in the next step.

(2) Evaluate crack depths using PSO

Based on Eq.(22), we have

$$(\alpha_1, \alpha_2, \dots, \alpha_n) = F^{-1}(\bar{f}_1, \bar{f}_2, \dots, \bar{f}_q) \quad (q \geq n) \quad (23)$$

From Eq. (23), we can see clearly that the inverse problem (Chaudhari and Maiti 2000, Dong *et al.* 2009, Lele and Maiti 2002, Li *et al.* 2005, Li and He 2011, Maiti and Patil 2004, Nandwana and Maiti 1997, Patil and Maiti 2003, 2005, Xiang *et al.* 2007a, 2008) to determine the depths of n cracks is essentially a discrete optimization problem. To estimate the depths of the n cracks from the crack depth detection database, PSO algorithm is employed to the crack depth and the first q natural frequencies are used as the inputs. Thus the following objective or fitness function to search for the “best fit” severities from the crack depth detection database as

$$\min \sum_{j=1}^q \left\| \frac{\bar{f}_m - \hat{f}_m}{\bar{f}_m} \right\|_2 \quad (24)$$

$$\text{subject to } 0.1 < \alpha_i < 0.9, \quad i = 1, 2, \dots, n \quad (25)$$

where $\|\cdot\|_2$ is the Euclidean norm (or the so-called 2-norm), $\bar{f}_m = F_m(\alpha_1, \alpha_2, \dots, \alpha_n)$ is the discrete function of the n damage depths $\alpha_i (i = 1, 2, \dots, n)$ (it is reflected by the crack depth detection database, as shown in Eq. (22)), constraint $0.1 < \alpha_i < 0.9$ limits the severity search space from 0.1 to 0.9, \hat{f}_m is the measured natural frequencies, where $m = 1, 2, \dots, q$. It notes that Eq. (25) is the constraint conditions.

3.3 Natural frequencies estimate formula updating

In most practice cases, the large difference between the measured frequencies \hat{f}_m and the computed f_m may make solutions irrelevant. For this reason, the ‘zero-setting’ procedure described by Adams (Adams *et al.* 1978) is adopted for model updating and hence reducing the difference. Zero-setting procedure is one of the output error methods and has found to be the most simple and suitable for crack detection in structures.

Consider Eqs.(1), (3), (14) and (15), it is known that the term $\phi_m \sum_{i=1}^n \frac{[v_m(x_i)]^2}{k_i}$ in Eq. (13) has no relation to Young’s modulus. From Eq. (16), the square of natural frequency for intact beam is linearly proportional to the Young’s modulus E . Therefore, we can use the zero-setting’ procedure to the intact beam to modified Young’s moduli

$$\frac{E}{\hat{E}_m} = \left(\frac{f_m}{\hat{f}_m}\right)^2 \tag{26}$$

where \hat{E}_m ($m = 1, 2, \dots, q$) is the corrected value of Young's modulus E , which can be obtained from Eq. (26) for each natural frequency. This procedure can greatly reduce the error between theoretical analysis and the experimental studies, which are caused by boundary conditions and material parameters.

After the above updating process, the resulting modified Young's moduli \hat{E}_m will be employed to calculate \hat{f}_m to construct the crack depth detection database.

4. Numerical simulation

In section 4.1, several examples in the literature are given to validate the approximate natural frequencies formula. The suggested simple crack detection method is also introduced in section 4.2.

4.1 The validity of approximate natural frequencies formula

4.1.1 Example 1 single crack

Taking the cracked cantilever beam for example, beam length $L = 0.5$ m, Young's modulus $E = 2.1 \times 10^{11}$ N/m², beam height and width are $h \times b = 0.02 \text{ m} \times 0.012$ m, Poisson's ratio $\mu = 0.3$ and material density $\rho = 7860$ kg/m³. Table 1 gives the first three natural frequencies using Eq. (13) and

Table 1 Comparison of Wavelet FEM and the present solution for cantilever beam

Case	β	α	Wavelet FEM (Xiang <i>et al.</i> 2008)			Present		
			\bar{f}_1/Hz	\bar{f}_2/Hz	\bar{f}_3/Hz	$\bar{f}_{p1}/\text{Hz} (\varepsilon_1)$	$\bar{f}_{p2}/\text{Hz} (\varepsilon_2)$	$\bar{f}_{p3}/\text{Hz} (\varepsilon_3)$
1	0	0	66.80	418.62	1172.15	66.80(0)	418.62(0)	1172.15(0)
2	0.1	0.1	66.38	417.65	1171.64	66.37(0.02)	417.64(0)	1171.63(0)
3	0.2	0.1	66.50	418.60	1170.60	66.50(0)	418.60(0)	1170.59(0)
4	0.2	0.3	64.24	418.47	1158.99	64.09(0.23)	418.46(0)	1158.06(0.08)
5	0.3	0.2	66.04	417.26	1156.12	66.03(0.02)	417.23(0.01)	1155.38(0.06)
6	0.3	0.3	65.07	415.55	1136.90	65.00(0.11)	415.38(0.04)	1133.09(0.34)
7	0.4	0.2	66.33	413.94	1163.82	66.3(0.05)	413.81(0.03)	1163.44(0.03)
8	0.4	0.4	64.77	399.47	1139.61	64.69(0.12)	396.98(0.62)	1133.00(0.58)
9	0.5	0.2	66.55	411.78	1172.14	66.54(0.02)	411.56(0.05)	1172.14(0)
10	0.5	0.4	65.68	390.84	1172.09	65.65(0.05)	386.89(1.01)	1172.08(0)
11	0.6	0.4	66.28	392.31	1132.26	66.27(0.02)	389.52(0.71)	1123.91(0.74)
12	0.6	0.6	65.37	356.18	1087.93	65.34(0.05)	337.59(5.22)	1037.81(4.61)
13	0.7	0.4	66.61	402.06	1089.16	66.61(0)	401.38(0.17)	1072.40(1.52)
14	0.7	0.6	66.29	375.87	996.40	66.28(0.02)	370.60(1.40)	894.38(10.24)
15	0.8	0.3	66.78	415.69	1139.81	66.78(0)	415.70(0)	1139.13(0.06)
16	0.8	0.8	66.57	386.44	912.33	66.57(0)	386.23(0.05)	806.46(11.6)

Note: Errors, and $\varepsilon_1 = |\bar{f}_{p1} - \bar{f}_1|/\bar{f}_1 \times 100\%$, $\varepsilon_2 = |\bar{f}_{p2} - \bar{f}_2|/\bar{f}_2 \times 100\%$ and $\varepsilon_3 = |\bar{f}_{p3} - \bar{f}_3|/\bar{f}_3 \times 100\%$

Table 2 Comparison of Wavelet FEM and the present solution for simply supported beam at two ends

Case	β	α	Wavelet FEM (Xiang <i>et al.</i> 2008)				Present		
			\bar{f}_1/Hz	\bar{f}_2/Hz	\bar{f}_3/Hz	$\bar{f}_{p1}/\text{Hz} (\varepsilon_1)$	$\bar{f}_{p2}/\text{Hz} (\varepsilon_2)$	$\bar{f}_{p3}/\text{Hz} (\varepsilon_3)$	
1	0	0	187.51	750.03	1687.56	187.51(0)	750.03(0)	1687.56(0)	
2	0.1	0.1	187.43	748.92	1682.85	187.43(0)	748.92(0)	1682.84(0)	
3	0.2	0.1	187.23	747.14	1681.14	187.23(0)	747.12(0)	1681.03(0.01)	
4	0.2	0.3	185.05	725.40	1636.37	185.01(0.02)	723.88(0.21)	1628.72(0.47)	
5	0.3	0.2	185.50	739.26	1685.02	185.48(0.01)	738.80(0.06)	1684.90(0.01)	
6	0.3	0.3	182.93	726.25	1681.99	182.78(0.08)	723.88(0.33)	1681.35(0.04)	
7	0.4	0.2	184.76	745.89	1678.25	184.70(0.03)	745.74(0.02)	1677.92(0.02)	
8	0.4	0.4	175.99	733.39	1650.37	174.89(0.63)	730.75(0.36)	1644.18(0.38)	
9	0.5	0.2	184.48	750.03	1661.01	184.40(0.04)	750.03(0)	1659.64(0.08)	
10	0.5	0.4	174.92	750.03	1585.83	173.56(0.78)	750.03(0)	1562.00(1.5)	

Note: Errors, and $\varepsilon_1 = |\bar{f}_{p1} - \bar{f}_1|/\bar{f}_1 \times 100\%$, $\varepsilon_2 = |\bar{f}_{p2} - \bar{f}_2|/\bar{f}_2 \times 100\%$ and $\varepsilon_3 = |\bar{f}_{p3} - \bar{f}_3|/\bar{f}_3 \times 100\%$

those by wavelet FEM (Xiang *et al.* 2008). From Table 1, under various crack location and crack depth, the numerical solutions are in agreement with the high precision wavelet FEM except for the large normalized crack depths, such as Cases 12, 14 and 16 in Table 1. It is well known that in actual structure, when crack depth attains $\alpha = 0.5$, the structure has breaking down. Therefore, the approximate natural frequency formula Eq. (13) is suitable to for crack detection use.

Changing the boundary conditions of cracked cantilever beam to simply supported at two ends. Table 2 also gives the first three natural frequencies solution of wavelet FEM (Xiang *et al.* 2008) and those of the present approximate method. The numerical performance of the present approximate method is similar to cantilever beam, and the present approximate method is very simple. In addition, for symmetric structures, it may obviously return to two symmetric positions. However, the search space of normalized crack location β should be restricted at interval $[0.1, 0.5]$ to gain a unique solution (Nandwana and Maiti 1997, Xiang *et al.* 2008). In the present crack detection method, for the crack locations are detected firstly using wavelet transform to decompose mode shape curvature, we can obtain the unique detection results for crack locations and depths.

4.1.2 Example 2 multiple cracks

Consider a damaged steel cantilever beam with two cracks. Its dimensions are: $L \times h \times b = 0.85 \text{ m} \times 0.02 \text{ m} \times 0.012 \text{ m}$. Material parameters are: Young's modulus $E = 2.06 \times 10^{11} \text{ N/m}^2$, Poisson's ratio $\mu = 0.3$ and density $\rho = 7860 \text{ kg/m}^3$.

The results calculated using Eq. (13) and FEM are presented in Table 3, where for each of the 14 crack cases, the first four frequencies are similar, then the present approximate equation is likely to be reliable.

In order to testify the validity of the approximate natural frequency estimation formula, a simply supported shaft with two cracks is also given and compared with FEM (Xiang and Liang 2011). The length L of the shaft is 0.85 m, the Young's modulus $E = 2.06 \times 10^{11} \text{ N/m}^2$, the cross-section radius $r_1 = 0.01 \text{ m}$, Poisson's ratio $\mu = 0.3$ and the material density $\rho = 7860 \text{ kg/m}^3$. Table 4 shows the first four natural frequencies of both the FEM and present approximate formula. As shown in Table 4, by comparing with FEM, the calculated values are in reasonably good agreement.

Table 3 Comparison of FEM and the present solution for cantilever beam with two cracks

α_2	α_1	β_2	β_1	FEM (Xiang and Liang 2011)				Present			
				\bar{f}_1/Hz	\bar{f}_2/Hz	\bar{f}_3/Hz	\bar{f}_4/Hz	\bar{f}_1/Hz	\bar{f}_2/Hz	\bar{f}_3/Hz	\bar{f}_4/Hz
0.2	0.3	0.3	0.1	22.02	141.51	397.54	785.18	21.96	141.40	397.38	784.67
0.2	0.4	0.3	0.1	21.41	140.19	396.86	785.13	21.25	139.74	396.49	784.58
0.2	0.3	0.4	0.2	22.26	142.49	397.40	771.70	22.25	142.46	397.11	770.79
0.3	0.3	0.4	0.2	22.15	141.26	395.46	769.16	22.13	141.17	394.78	768.62
0.4	0.3	0.4	0.2	21.97	139.36	392.46	765.50	21.92	139.07	390.97	765.08
0.2	0.5	0.5	0.3	21.71	140.24	379.90	764.84	21.63	139.85	375.31	760.62
0.3	0.5	0.5	0.3	21.66	138.59	379.78	754.99	21.56	137.96	375.30	750.43
0.4	0.5	0.5	0.3	21.58	136.11	379.60	740.76	21.45	134.88	375.30	733.83
0.4	0.4	0.6	0.4	22.37	134.51	384.94	775.46	22.36	133.24	384.09	772.98
0.5	0.4	0.6	0.4	22.31	131.26	379.05	772.25	22.28	128.91	376.92	767.92
0.6	0.4	0.6	0.4	22.20	127.00	372.02	768.37	22.17	122.77	366.73	760.73
0.1	0.3	0.7	0.5	22.78	140.11	400.56	769.93	22.77	139.95	400.54	768.59
0.1	0.2	0.7	0.5	22.84	141.87	400.56	779.11	22.84	141.84	400.55	778.78
0.1	0.4	0.7	0.5	22.66	137.40	400.55	756.56	22.66	136.87	400.54	751.99

Table 4 Comparison of FEM and the present solution for a shaft with two cracks

α_2	α_1	β_2	β_1	FEM (Xiang and Liang 2011)				Present			
				\bar{f}_1/Hz	\bar{f}_2/Hz	\bar{f}_3/Hz	\bar{f}_4/Hz	\bar{f}_1/Hz	\bar{f}_2/Hz	\bar{f}_3/Hz	\bar{f}_4/Hz
0.2	0.3	0.3	0.1	55.40	220.94	498.69	884.35	55.34	220.10	495.20	875.34
0.2	0.4	0.3	0.1	55.34	220.18	495.47	876.32	55.24	218.70	489.23	860.66
0.2	0.3	0.4	0.2	55.24	218.83	489.77	862.92	55.03	218.83	492.38	880.41
0.3	0.3	0.4	0.2	55.04	218.97	492.75	881.30	54.51	218.05	490.61	872.20
0.4	0.3	0.4	0.2	54.54	218.31	490.92	873.75	53.60	216.65	487.46	857.53
0.2	0.5	0.5	0.3	53.70	217.22	487.70	861.84	53.30	211.51	495.13	873.47
0.3	0.5	0.5	0.3	53.42	212.91	495.47	875.53	52.73	211.51	490.03	873.47
0.4	0.5	0.5	0.3	52.94	212.86	490.50	875.40	51.72	211.51	480.90	873.47
0.4	0.4	0.6	0.4	52.46	217.43	490.57	840.38	52.17	217.28	488.89	834.71
0.5	0.4	0.6	0.4	51.63	215.99	488.01	828.08	51.14	215.71	485.34	818.20
0.6	0.4	0.6	0.4	48.66	211.27	479.70	793.71	47.10	209.54	471.47	753.61
0.1	0.3	0.7	0.5	54.71	222.38	493.06	890.23	54.70	222.36	492.60	890.05
0.1	0.2	0.7	0.5	55.26	222.35	497.82	890.23	55.26	222.36	497.71	890.05
0.1	0.4	0.7	0.5	53.78	222.37	485.13	890.17	53.68	222.36	483.48	890.05

In addition, Table 5 shows the comparison of analytical solution (Lee 2009) with those of the present computing for a cantilever beam with three cracks. The geometry and material parameters are similar to *Example 1*. Suppose the three normalized crack depths α_1 , α_2 and α_3 are fixed to 0.1, four crack cases are compared. The results of the first six natural frequencies are matched well.

By summarizing the above natural frequency analyze and comparisons, the above results of several single and multiple cracked beam and shaft examples indicate that reasonably good calculation

Table 5 Comparison of analytical solution and the present solution for a cantilever beam with three cracks (0.1)

Method	β_1	β_2	β_3	\bar{f}_1/Hz	\bar{f}_2/Hz	\bar{f}_3/Hz	\bar{f}_4/Hz	\bar{f}_5/Hz	\bar{f}_6/Hz
Analytical solution (Lee 2009)	0.2	0.4	0.6	66.35063	415.7231	1165.632	2284.937	3754.451	5666.543
	0.2	0.4	0.8	66.37799	417.0456	1164.765	2275.911	3756.103	5661.717
	0.2	0.6	0.8	66.46774	416.6172	1164.288	2275.992	3756.291	5661.737
	0.4	0.6	0.8	66.64503	415.4261	1163.551	2281.916	3752.092	5665.596
Present	0.2	0.4	0.6	66.34607	415.6844	1165.559	2284.765	3753.596	5666.377
	0.2	0.4	0.8	66.37395	417.0335	1164.668	2275.551	3755.223	5661.459
	0.2	0.6	0.8	66.46532	416.6048	1164.145	2275.689	3755.391	5661.469
	0.4	0.6	0.8	66.64466	415.3773	1163.457	2281.723	3751.172	5665.393

accuracy can be achieved for the crack problems by the proposed approximate natural frequency estimation formula. The main advantage of the proposed formula is that it is very simple.

4.2 Crack detection for simply supported beam at two ends (shaft) with three cracks

Suppose the beam dimensions and the material properties are: $L = 1\text{m}$, $b \times h = 0.02\text{ mm} \times 0.04\text{ mm}$, Young's modulus $E = 2.06 \times 10^{11}\text{ N/m}^2$, material density $\rho = 7860\text{ kg/m}^3$, and Poisson's ratio $\mu = 0.3$. Crack case is considered as: $\beta_1 = 0.1$, $\beta_2 = 0.3$, $\beta_3 = 0.4$ and $\alpha_1 = \alpha_2 = \alpha_3 = 0.1$.

The first modal shape is calculated by 60 BSWI₄₃ (4 and subscript 3 denote the order and the level of B-spline wavelet on the interval, BSWI) beam elements (Xiang *et al.* 2007b), as shown in Fig. 3(a). The horizontal coordinate of each subplot denotes the relative location β . Using Db6 wavelet (Daubechies wavelet with six vanishing moment) (Mallat 1999) to decompose the first mode shape (signal) at one level, the approximation signal and the detailed signal are show in Figs. 3(b) and (c), respectively. From Fig. 3(c), we can see clearly that the boundary distortion phenomenon is occurred at both the edge of detailed signal. This phenomenon will significantly influence the identification of crack locations. However, when we calculate the first mode shape curvature using

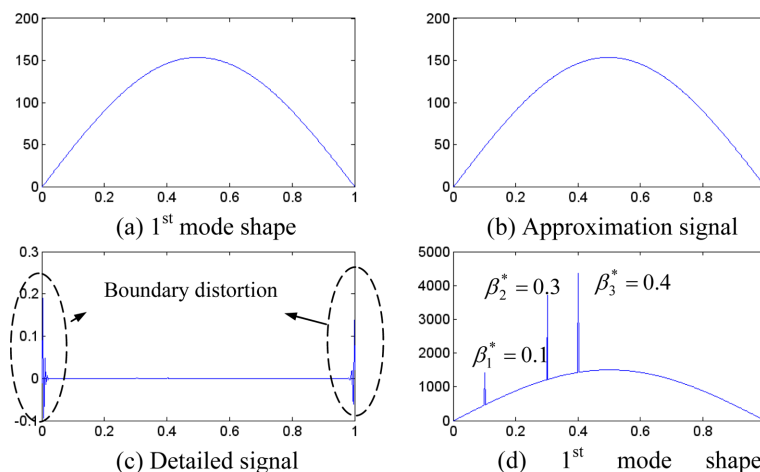


Fig. 3 Crack location detection using the first mode shape and the first mode shape curvature

Table 6 The first three noise-free natural frequencies calculated by the approximate formula

Case	Crack depths			Noise-free natural frequencies (Hz)		
	α_1	α_2	α_3	\bar{f}_1	\bar{f}_2	\bar{f}_3
1	0.1	0.2	0.2	32.25	203.75	567.59
2	0.2	0.3	0.3	30.83	198.26	550.08
3	0.2	0.3	0.1	31.31	203.20	559.01
4	0.3	0.3	0.1	30.23	200.70	557.67
5	0.4	0.3	0.1	28.47	196.62	555.50
6	0.3	0.4	0.1	29.40	199.21	539.68
7	0.3	0.4	0.3	28.92	194.27	530.75
8	0.3	0.4	0.4	28.42	189.10	521.41
9	0.5	0.5	0.1	23.68	186.61	506.67
10	0.5	0.5	0.2	23.50	184.84	503.47

Eq. (21), we the three peaks indicate the detected crack locations, i.e., $\beta_1^* = 0.1$, $\beta_2^* = 0.3$, $\beta_3^* = 0.4$ and the predications for the three damage locations are 100% accurate. Therefore, the locations of the three cracks can be detected accurately by looking at peaks from the curve modal shape. It is note that, in our investigation, any order of mode shape curvature can obtain the similar results. However, the crack depths cannot be determined directly from the mode shape curvature.

As mentioned in Section 3.2, to detect three crack depths, three natural frequencies \bar{f}_1 , \bar{f}_2 and \bar{f}_3 are the necessary condition to obtain a robust solution of unknown α_1^* , α_2^* and α_3^* . Because the three crack locations $\beta_1^* = 0.1$, $\beta_2^* = 0.3$ and $\beta_3^* = 0.4$ are detected, we focus on the evaluation of crack depths at the three crack locations. We consider eight different depth combinations as specified by different $(\alpha_1, \alpha_2, \alpha_3)$ groups in Table 6 and the first three noise-free natural frequencies \bar{f}_1 , \bar{f}_2 , \bar{f}_3 calculated by Eq. (13) are also given in the same table. Eq. (13) is also applied to obtain crack depth detection database, α_1 , α_2 and α_3 are varied from 0.1 to 0.9 with step length of 0.01. Therefore, there are 531441 ($=81 \times 81 \times 81$) data points in the search space of the discrete functions $\bar{f}_m = F_m(\alpha_1, \alpha_2, \alpha_3)$, where $m = 1, 2, 3$.

To simulate noise-contaminated signals, artificial white Gaussian noise (WGN) is added (Suk and Gillis 2005). This is done using the random number generator, *randn* (pseudorandom values drawn from the standard normal distribution) in software MATLAB7.10 as

$$\bar{f}_m^N = (1 + nl \times \text{randn}) \times \bar{f}_m \quad (27)$$

where nl is the noise level, and \bar{f}_m^N is the noisy frequency.

Suppose $nl=2\%$, the first three noise-contaminated natural frequencies are shown in Table 7. The optimization is implemented with MATLAB using a PSO Toolbox coded by Birge (Birge 2003). More information about the Toolbox can be found in its help documents.

In this investigation, a population of 50 individuals is used as particles. According to the recommendations by Birge (Birge 2003), the values of the cognition learning and the social learning factors c_1 and c_2 are set to 2, the maximum particle fly speed is fixed at 10% of the range of α_1 , α_2 and α_3 , i.e., $0.1 \times (0.9 - 0.1) = 0.08$. The value of inertia weight w decreases linearly from 0.9 in the first iteration to 0.4 for the 100th iteration. The convergence is reached long before 100 iterations. Because the PSO is for continuous variable optimization problems, the α_1 , α_2 and α_3 values provided

Table 7 The first three noise-contaminated natural frequencies and crack depths evaluation results

Case	Noise-free natural frequencies(Hz)			Predicted crack depths		
	\bar{f}_1^N	\bar{f}_2^N	\bar{f}_3^N	$\alpha_1^*(\varepsilon_1)$	$\alpha_2^*(\varepsilon_2)$	$\alpha_3^*(\varepsilon_3)$
1	32.96	203.84	579.15	0.123(2.3)	0.233(3.3)	0.228(2.8)
2	30.66	197.22	548.61	0.199(0.1)	0.369(6.9)	0.338(3.8)
3	31.75	196.09	551.02	0.227(2.7)	0.344(4.4)	0.120(2.0)
4	28.99	199.55	572.74	0.339(3.9)	0.348(4.8)	0.120(2.0)
5	28.27	193.35	553.00	0.453(5.3)	0.336(3.6)	0.120(2.0)
6	28.92	195.31	533.32	0.347(4.7)	0.453(5.3)	0.100(0.0)
7	28.01	189.78	527.63	0.323(2.3)	0.499(9.9)	0.301(0.1)
8	28.71	187.08	512.57	0.259(4.1)	0.501(10.1)	0.464(6.4)
9	23.81	179.14	495.32	0.541(4.1)	0.573(7.3)	0.110(1)
10	23.52	188.40	528.91	0.536(3.6)	0.598(9.8)	0.152(4.8)

Note: Errors, and $\varepsilon_1 = |\alpha_1 - \alpha_1^*| \times 100\%$, $\varepsilon_2 = |\alpha_2 - \alpha_2^*| \times 100\%$ and $\varepsilon_3 = |\alpha_3 - \alpha_3^*| \times 100\%$

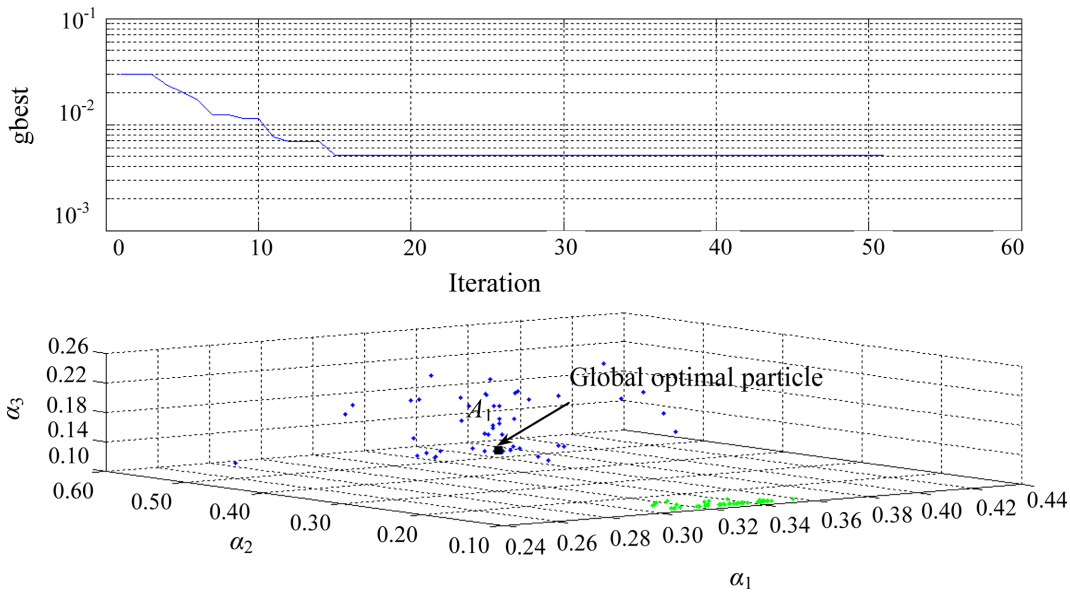


Fig. 4 The PSO convergence progress and the optimal particle location

by the PSO algorithm may not be discrete. Therefore, the α_1 , α_2 and α_3 outputs in each iteration should be rounded up and down to the nearest discrete numbers. More specifically, α_1 , α_2 and α_3 are rounded to the nearest value available in the severity evaluation database.

Fig. 4 shows the search convergence process and the global optimization particle locations for one case, i.e., the crack depth detection results for case 6 (as shown in Table 7) using the first three noise-contaminated frequencies \bar{f}_1^N , \bar{f}_2^N and \bar{f}_3^N . From the upper figures in Fig. 4, the PSO algorithms achieve the best solutions in less than 15 iterations. From the bottom figures in Fig. 4, we can see clearly that the global optimization particles are located at point A_1 ($\alpha_1^* = 0.347$, $\alpha_2^* = 0.453$ and $\alpha_3^* = 0.100$). The results are summarized in Tables 7. As shown in the table, with \bar{f}_1^N , \bar{f}_2^N and \bar{f}_3^N ,

the evaluation errors for depth of α_1^* , α_2^* and α_3^* are in the range of 0.0% to 10.1%.

The above example clearly demonstrates that the proposed method can detect the locations and depths of cracks reasonably well for measurements with lower level noise content. The two-step hybrid method provides for a possibly more reliable crack detection strategy.

5. Experimental investigation

We shall now concentrate on the experimental validation. The experimental setup is shown in Fig. 5. The test system consists of a cantilever beam with two cracks, an accelerometer, an impact hammer, a signal conditioner, NI data acquisition card and a computer with fast Fourier transform (FFT) program. The geometry of the cantilever beam are $L \times h \times b = 0.5 \text{ m} \times 0.019 \text{ m} \times 0.012 \text{ m}$. The cantilever material is structural steel with Young's modulus $E = 2.06 \times 10^{11} \text{ N/m}^2$, Poisson's ratio $\mu = 0.3$ and density $\rho = 7860 \text{ kg/m}^3$.

The experiments are conducted using two beams, one intact and the other with two cracks. The locations and depths of the two cracks are respectively $e_1 = 80 \text{ mm}$, $e_2 = 380 \text{ mm}$, $c_1 = 8 \text{ mm}$ and $c_2 = 8 \text{ mm}$. Therefore, the respective normalized crack locations and depths are $\beta_1 = 0.16$, $\beta_2 = 0.76$, $\alpha_1 = 0.42$ and $\alpha_2 = 0.42$. As we known, in a typical impact test, the accelerometer is attached to a single point on the beam (in the present, the accelerometer is fixed near the left end of the beam),

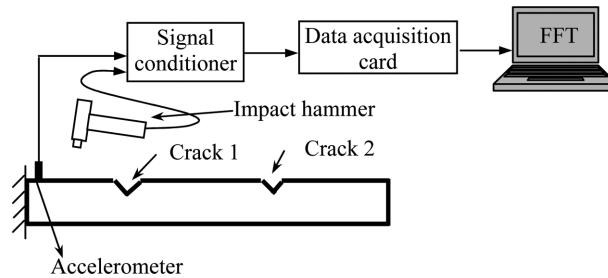


Fig. 5 Experimental setup

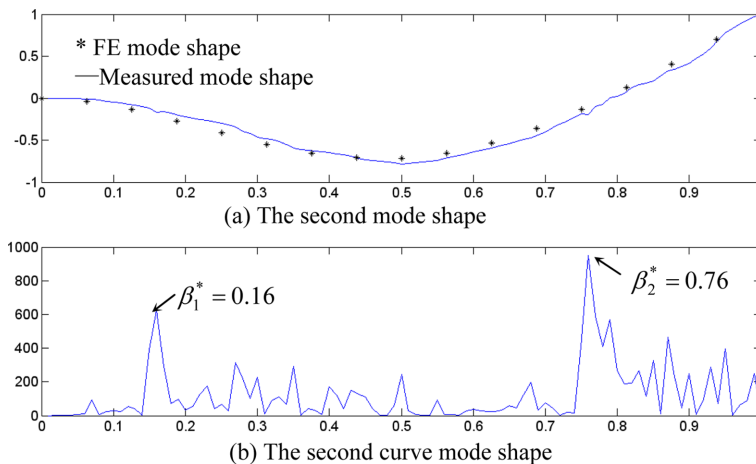


Fig. 6 Two crack locations detection using the second mode shape curvature

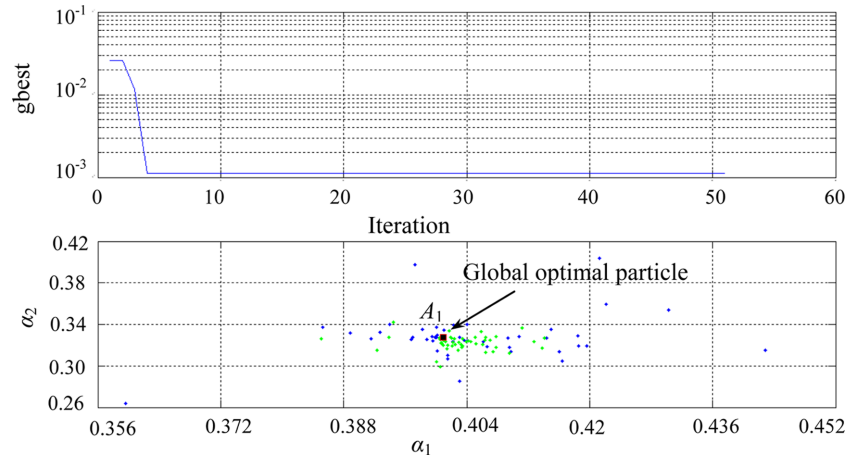


Fig. 7 The PSO convergence progress and the optimal particle location represented two crack depths

and the hammer is used to impact it as many points to define its mode shape. In the experimental study, the sampling frequency f_s is 5,000 Hz and 10,000 data points are collected at each impact points. The first three measured frequencies are: $\hat{f}_1 = 58.5$ Hz, $\hat{f}_2 = 345$ Hz and $\hat{f}_3 = 906$ Hz for intact beam; $\hat{f}_1^c = 54$ Hz, $\hat{f}_2^c = 337.5$ Hz and $\hat{f}_3^c = 869.5$ Hz for cracked beam. The analytical solution of intact beam using Eq. (13) are: $f_1 = 62.85$ Hz, $f_2 = 393.88$ Hz and $f_3 = 1102.89$ Hz. Therefore, the values of corrected Young's modulus calculated by Eq. (25) are: $\hat{E}_1 = 1.7847 \times 10^{11}$, $\hat{E}_2 = 1.5804 \times 10^{11}$ and $\hat{E}_3 = 1.3901 \times 10^{11}$.

Fig. 6 shows the second modal shape and the mode shape curvature. The asterisk and solid line in Fig. 6(a) denote the FE modal shape and the measured result. Compared with FE results, some errors are inevitably introduced into measured modal shape by measurement environments. In Fig. 6(b), the horizontal coordinate represents β and the peak points at $\beta_1^* = 0.16$ and $\beta_2^* = 0.76$ reveal the exact locations of the two cracks.

Using \hat{E}_m ($m=1, 2, 3$) and Eq.(13), we can obtain three function relationships between the first three frequencies and the two crack depths (crack depth detection databases). α_1 and α_2 are varied from 0.1 to 0.9 with step length of 0.01. Therefore, there are 6561 ($=81 \times 81$) data points in the search space of the discrete functions $\bar{f}_m = F_m(\alpha_1, \alpha_2)$, where $m = 1, 2$. Similar to the simulation example on how to use PSO algorithm, we can search for the global optimization particles are located at point A_1 ($\alpha_1^* = 0.401$, $\alpha_2^* = 0.328$) in Fig. 7 provides the estimated crack depths. The relative errors between the estimated and the actual depths are $\varepsilon_1 = |\alpha_1^* - \alpha_1| \times 100\% = 1.9\%$ and $\varepsilon_2 = |\alpha_2^* - \alpha_2| \times 100\% = 9.2\%$. As shown above, the crack location predictions are 100% accurate for the given cases whereas the relative errors of crack depth estimations are within 9.2%. Hence, the proposed simple crack detection method can be used for real applications with reasonable accuracy.

6. Conclusions

This paper suggests a simple procedure for crack detection in beam-like structures which is based on mode shape curvature and few estimated natural frequencies of the beam and no finite element model is needed. The procedure involves two steps. The first step is the application of mode shape

curvature to detect the possibly existence and locations of cracks in beam-like structures. The second step is the employment of particle swarm optimization to evaluate crack depths from the crack depth detection database (the relationship of natural frequencies and crack depths). In the present method, we use Rayleigh quotient to estimate the approximate natural frequencies of beam-like structures under different boundary conditions. Therefore, the relationship of natural frequencies and crack depths can be easily constructed by a simple formula. The numerical and the experimental results show that the present method will not just detect crack locations and depths but will also distinguish the intact and cracked beams. It should be noted that the complex finite element solution is not needed in practice application. The basic idea of this method is being developed for plate structures or more complicated plane/spatial frame structures.

Acknowledgements

The authors are grateful to the support of Japan Society for the Promotion of Science (ID: P11052) and the National Science Foundation of China (Nos. 51175097, 51105085, 51165003). GuangXi key Technologies R&D Program of China (Nos. 1099022-1, 10123005-12). This material is also based upon work funded by Zhejiang Technologies R&D Program of China (No. 2010C31094) and Zhejiang Provincial Natural Science Foundation of China under Grant No.Y1110046.

References

- Adams, R.D., Cawley, P., Pye, C.J. and Stone, B.J. (1978), "A vibration technique for non-destructively assessing the integrity of structures", *J. Mech. Eng. Sci.*, **20**(2), 93-100.
- Amiri, G.G., Razzaghi, S.A.S. and Bagheri, A. (2011), "Damage detection in plates based on pattern search and Genetic algorithms", *Smart Struct. Syst.*, **7**(2), 117-132.
- Begambre, O. and Laier, J.E. (2009), "A hybrid particle swarm optimization-simplex algorithm (PSOS) for structural crack identification", *Adv. Eng. Softw.*, **40**(9), 883-891.
- Birge, B. (2003), "PSOt-a particle swarm optimization toolbox for use with Matlab", *In: Proceedings of the IEEE Swarm Intelligence Symposium (SIS03)*.
- Chaudhari, T.D. and Maiti, S.K. (2000), "A study of vibration of geometrically segmented beams with and without crack", *Int. J. Solids. Struct.*, **37**(5), 761-779.
- Chen, X.F., He, Z.J. and Xiang, J.W. (2005), "Experiments on crack identification in cantilever beams", *Exp. Mech.*, **45**(3), 295-300.
- Chen, X.F., Zi, Y.Y., Li, B. and He, Z.J. (2006), "Identification of multiple cracks using a dynamic meshrefinement method", *J. Strain Anal. Eng.*, **41**(1), 31-39.
- Higham, D.J. and Higham, N.J. (2005), *MATLAB Guide*, 2nd Ed., New York, Society for Industrial and Applied Mathematics.
- Dong, H.B., Chen, X.F., Li, B., He, Z.J. (2009), "Rotor crack detection based on highprecision modal parameter identification method and wavelet finite element model", *Mech. Syst. Signal. Pr.*, **23**, 69-883.
- Fan, W. and Qiao, P.Z. (2011), "Vibration-based damage identification methods: a review and comparative study", *Struct. Health Monit.*, **10**(1), 83-111.
- Fourie, P.C. and Groenwold, A.A. (2002), "The particle swarm optimization algorithm in size and shape optimization", *Struct. Multidiscip. O.*, **23**(4), 259-267.
- Gokdag, H. (2010), "A new structural damage detection index based on analyzing vibration modes by the wavelet transform", *Struct. Eng. Mech.*, **35**(2), 257-260.
- Gokdag, H. (2011), "Wavelet-based damage detection method for a beam-type structure carrying moving mass",

- Struct. Eng. Mech.*, **38**(1), 81-97.
- Harris, C.M. and Piersol, A.G. (2002), *Harris' Shock and Vibration Handbook*, 5th Ed., New York, McGraw-Hill.
- Kennedy, J. and Eberhart, R. (1995), "Particle swarm optimization", *Proceedings of IEEE International Conference on Neural Networks*, Perth, Australia.
- Kim, J.T., Park, J.H., Yoon, H.S. and Yi, J.H. (2007), "Vibration-based damage detection in beams using genetic algorithm", *Smart Struct. Syst.*, **3**(3), 263-280.
- Kim, J.T., Park, J.H., Koo, K.Y. and Lee, J.J. (2008), "Acceleration-based neural networks algorithm for damage detection in structures", *Smart Struct. Syst.*, **4**(5), 583-603.
- Koo, K.Y., Lee, J.J., Yun, C.B. and Kim, J.T. (2008), "Damage detection in beam-like structures using deflections obtained by modal flexibility matrices", *Smart Struct. Syst.*, **4**(5), 605-628.
- Lakshmanan, N., Raghuprasad, B.K., Muthurani, K., Gopalakrishnan, N. and Basu, D. (2008), "Identification of reinforced concrete beam-like structures subjected to distributed damage from experimental static measurements", *Comput. Concrete*, **5**(1), 37-60.
- Lee, J.H. (2009), "Identification of multiple cracks in a beam using natural frequencies", *J. Sound. Vib.*, **320**(3), 482-490.
- Lele, S.P. and Maiti, S.K. (2002), "Modeling of transverse vibration of short beams for crack detection and measurement of crack extension", *J. Sound. Vib.*, **257**(3), 559-583.
- Li, B. Chen, X.F. and He, Z.J. (2005), "Detection of crack location and size in structures using wavelet finite element methods", *J. Sound. Vib.*, **285**(4-5), 767-782.
- Li, B. and He, Z.J. (2011), "Frequency-based crack identification for static beam with rectangular cross-section", *J. Vibroeng.*, **13**(3), 477-486.
- Liang, R.Y., Choy, F.K. and Hu, J. (1991), "Frequency-based crack identification for static beam with rectangular cross-section", *J. Franklin I.*, **328**(4), 505-518.
- Liang, R.Y., Hu, J. and Choy, F.K. (1992a), "Theoretical study of crack-induced eigenfrequency changes on beam structures", *J. Eng. Mech.-ASCE*, **118**(2), 384-396.
- Liang, R.Y., Hu, J. and Choy, F.K. (1992b), "A quantitative NDE technique for assessing damage in beam structures", *J. Eng. Mech.-ASCE*, **118**(7), 1468-1487.
- Hu, J. and Liang, R.Y. (1993), "An integrated approach to detection of cracks using vibration characteristics", *J. Franklin I.*, **330**(5), 841-853.
- Maiti S.K. and Patil, D.P. (2004), "A method of analysis for detection of multiple cracks in beams based on vibration", *Adv. Vib. Eng.*, **3**(4), 348-369.
- Mallat, S.G. (1999). *A Wavelet Tour of Signal Processing*, New York: Academic Press.
- Mendrok, K. and Uhl, T. (2010), "The application of modal filters for damage detection", *Smart Struct. Syst.*, **6**(2), 115-133.
- Montejo, L.A. (2011), "Signal processing based damage detection in structures subjected to random excitations", *Struct. Eng. Mech.*, **40**(6).
- Nandwana, B.P. and Maiti, S.K. (1997), "Detection of the location and size of a crack in stepped cantilever beams based on measurements of natural frequencies", *J. Sound. Vib.*, **203**(3), 435-446.
- Ostachowicz, W.M. and Krawczuk (1991), "Analysis of the effect of cracks on the natural frequencies of a cantilever beam", *J. Sound Vib.*, **150**(2), 191-201.
- Pandey, A.K., Biswas, M. and Samman, M.M. (1991), "Damage detection from changes in curvature mode shapes", *J. Sound Vib.*, **145**(2), 321-332.
- Papadopoulos, C.A. and Dimarogonas, A.D. (1987), "Coupled longitudinal and bending vibrations of a rotating shaft with an open crack", *J. Sound. Vib.*, **117**(1), 81-93.
- Patil, D.P. and Maiti, S.K. (2003), "Detection of multiple cracks using frequency measurements", *Eng. Fract. Mech.*, **70**(12), 1553-1572.
- Patil, D.P. and Maiti, S.K. (2005), "Experimental verification of a method of detection of multiple cracks in beams based on frequency measurements", *J. Sound Vib.*, **281**(1-2), 439-451.
- Rajasekaran, S. and Varghese, S.P. (2005), "Damage detection in beams and plates using wavelet transforms", *Comput. Concrete*, **2**(6), 481-498.
- Shi, Y.H. and Eberhart, R. (1998), "A modified particle swarm optimizer", *Proceedings of the IEEE International*

- Conference on Evolutionary Computation*, Anchorage, USA.
- Shih, H.W., Thambiratnam, D.P. and Chan, T.H.T. (2009) "Vibration based structural damage detection in flexural members using multi-criteria approach", *J. Sound Vib.*, **323**(3-5), 645-661.
- Shih, H.W., Thambiratnam, D.P. and Chan, T.H.T. (2011), "Damage detection in truss bridges using vibration based multi-criteria approach", *Struct. Eng. Mech.*, **39**(2), 187-206.
- Sinou, J.J. (2007), "A robust identification of single crack location and size only based on pulsations of the cracked system", *Struct. Eng. Mech.*, **25**(6), 691-716.
- Suk, M. and Gillis, E.D. (2005), "Effect of mechanical design of the suspension on dynamic loading process", *Microsyst. Technol.*, **11**(8-10), 846-850.
- Tada, H., Paris, P.C. and Irwin, G.R. (2000), *The Stress Analysis of Cracks Handbook*, 3rd Ed., New York, The American Society of Mechanical Engineers.
- Timoshenko, S., Young, D.H. and Weaver, W. (1974), *Vibration Problems in Engineering*, 4th Ed., London, John Wiley and Sons.
- Xiang, J.W., Chen, X.F., Mo, Q.Y. and He, Z.J. (2007a), "Identification of crack in a rotor system based on wavelet finite element method", *Finite. Elem. Anal. Des.*, **43**(14), 1068-1081.
- Xiang, J.W., Chen, X.F., He, Z.J. and Zhang, Y.H. (2007b), "The construction of 1D wavelet finite elements for structural analysis", *Comput. Mech.*, **40**(2), 325-339.
- Xiang, J.W., Zhong, Y.T., Chen, X.F. and He, Z.J. (2008), "Crack detection in a shaft by combination of waveletbased elements and genetic algorithm", *Int. J. Solids. Struct.*, **45**(17), 4782-4795.
- Xiang, J.W., Chen, X.F. and Yang, L.F. (2009), "Crack identification in short shafts using wavelet-based element and neural network", *Struct. Eng. Mech.*, **33**(5), 571-589.
- Xiang, J.W., Wang, Y.X., Jiang, Z.S. and Chen, X.F. (2011a), "Study on damage detection software of beam-like structures", *Struct. Eng. Mech.*, **39**(1), 77-91.
- Xiang, J.W. and Liang, M. (2011), "Multiple damage detection method for beams based on multi-scale elements using Hermite cubic spline wavelet", *CMES-Comput. Model. Eng. Sci.*, **73**(3), 267-298.
- Yun, G.J., Ogorzalek, K.A., Dyke, S.J. and Song, W. (2009), "A two-stage damage detection approach based on subset selection and genetic algorithms", *Smart Struct. Syst.*, **5**(1), 1-21.
- Zhong, Y. and Ye, Z.F. (2009), "Particle swarm optimisation algorithm for crack shape reconstruction in magnetic flux leakage nondestructive testing", *Nondestruct. Test. Eva.*, **24**(1-2), 243-250.